Unipolar Resistive Switching Characteristics of a ZrO_2 Memory Device With Oxygen Ion Conductor Buffer Layer

Dai-Ying Lee and Tseung-Yuen Tseng, *Fellow, IEEE*

***Abstract*—Oxygen ion migration is an important factor in the formation and rupture of a conducting filament to cause resistive switching (RS) behavior. A calcium oxide-doped zirconium oxide ($CaO:ZrO_2$) oxygen ion conductor buffer layer is introduced between the Ti/ZrO_2 interface of conventional Ti/ZrO_2/Pt memory devices to improve their unipolar RS properties. Increasing the CaO doping concentration to 2 mol% introduces higher oxygen vacancy content within the $CaO:ZrO_2$ buffer layer, leading to higher oxygen ion conductivity. This allows more oxygen ions to migrate from the oxygen reservoir laterally and vertically across the 2-mol% $CaO:ZrO_2$ buffer layer to the region where the conducting filament forms and ruptures. Therefore, the Ti/2-mol% $CaO:ZrO_2$/ZrO_2/Pt device in this letter exhibits good endurance, high-speed switching (50 ns) without soft errors, stubborn nondestructive readout, and stable retention at 150 °C.**

***Index Terms*—Oxygen ion migration, resistive random access memory (RRAM), unipolar switching, ZrO_2 film.**

I. Introduction

DUE to the advantages of a simple structure, low power consumption, high-speed operation, high-density capacity, and easy-integration processing, resistive random access memory (RRAM) has attracted intensive studies. RRAM uses two distinguishable resistive states (low resistive state, ON state and high resistive state, OFF state) to store digital data in a memory cell. By applying an electric field on the cell, these two memory states can be continuously switched back and forth. However, an important issue to be overcome in practical RRAM applications is how to avoid the resistive switching (RS) operation failure phenomenon during successive RS cycles. When switching to ON state or OFF state, the memory cell does not transiently respond to the applied electric field, and the memory state remains unchanged [1], [2]. Such soft errors may cause data loss or store the wrong data. Inserting a buffer layer between the resistive layer and the electrode can stabilize the RS operation. For example, introducing an oxygen-gettering-material Ti or a conducting IrO_2 thin layer to the metal/insulator interface stabilizes the local oxygen ion migration for the conducting filament formation/rupture [2]–[4]. Because oxygen ion migration causes reduction and reoxidation in certain regions of the conducting filament, it is proposed to determine the RS mechanism [5]–[7]. Previous research shows that the strong oxygen-gettering ability of Ti forms a native ZrO_y interface layer between the Ti top electrode and ZrO_2. The interface layers consist of an oxidized Ti layer (TiO_z, an oxygen reservoir) and an approximately 5-nm-thick oxygen-deficient ZrO_2 (ZrO_y) layer [6]–[8]. After a forming process, the conducting filament composed of the oxygen vacancies is formed in series with the interface layers, leading to be switched to ON state. To reach OFF state, the oxygen ions migrate from the TiO_z layer, then pass the ZrO_y layer, and finally reoxidize the region of the conducting filament near the ZrO_y layer. Oxygen ion consumption in the interface layers leads to unstable unipolar RS and poor endurance properties [7]. Consequently, a modified bias operation is further adopted to improve the endurance cycles by minimizing the oxygen ion consumption [9].

In this letter, we introduce a calcium oxide-doped zirconium oxide ($CaO:ZrO_2$) buffer layer to replace the native ZrO_y between the ZrO_2 memory film and the Ti top electrode. $CaO:ZrO_2$ is a well-known oxygen ion conductor that allows oxygen ions to migrate easily and quickly. The ZrO_2-based memory devices with the $CaO:ZrO_2$ buffer layer have better RS properties than those without the buffer layer.

II. Experiments

A 30-nm-thick ZrO_2 film was deposited on the Pt/Ti/SiO_2/Si substrates from a ZrO_2 ceramic target at 200 °C by an RF magnetron sputter. The base pressure of the sputtering chamber was below 5×10^{-6} torr, and the working pressure was 10 mtorr. The pressure was maintained by a 1 : 2 ratio mixture of oxygen and argon gas at a flow of 18 sccm. The RF power density was fixed at 2.63 W/cm^2. Then, 0-, 0.4-, 1.2-, 2-, and 2.8-mol% $CaO:ZrO_2$ buffer layers with a 5-nm thickness were deposited on the as-deposited ZrO_2 films from various composition $CaO:ZrO_2$ ceramic targets by an RF magnetron sputter under the same procedures as the preparation of ZrO_2 films. Finally, a 150-nm-thick Ti top electrode was formed by electron beam evaporation at ambient temperature. This electrode had a diameter of 250 μm patterned by a shadow mask to complete the Ti/$CaO:ZrO_2$/ZrO_2/Pt devices. On a separate experiment, the $CaO:ZrO_2$ thin films with a thickness of 60 nm were prepared

Manuscript received February 13, 2012; revised March 3, 2012; accepted March 21, 2012. Date of publication May 7, 2012; date of current version May 18, 2012. This work was supported by the National Science Council of Taiwan under Project NSC 99-2221-E-009-166-MY3. The review of this letter was arranged by Editor T. San.

The authors are with the Department of Electronics Engineering and the Institute of Electronics, National Chiao Tung University, Hsinchu 300, Taiwan (e-mail: tseng@cc.nctu.edu.tw).

Color versions of one or more of the figures in this letter are available online at http://ieeexplore.ieee.org.

Digital Object Identifier 10.1109/LED.2012.2192252

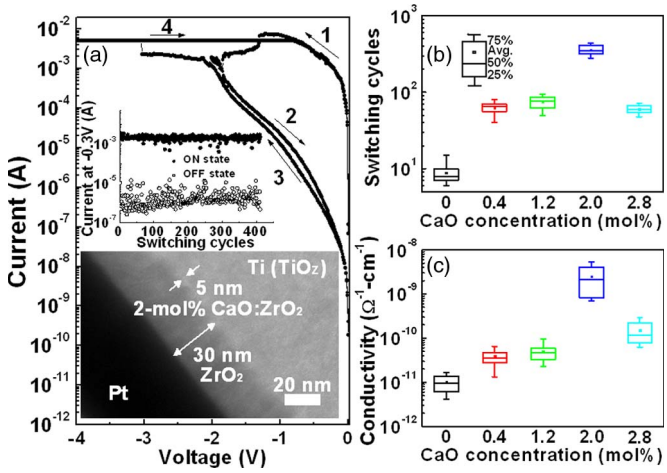

Fig. 1. (a) Typical unipolar RS I–V curve of the Ti/CaO:ZrO_2/ZrO_2/Pt device. The insets show the cross-sectional TEM image and the endurance cycles of the Ti/CaO:ZrO_2/ZrO_2/Pt device, respectively, where the CaO concentration is 2 mol%. (b) Endurance cycles for the Ti/CaO:ZrO_2/ZrO_2/Pt devices varied with CaO concentration of the buffer layers. (c) Electrical conductivity of the CaO:ZrO_2 buffer layer changes with CaO concentration.

on Pt/Ti/SiO_2/Si substrates following the same procedures. After depositing a Pt top electrode, the electrical conductivity values of the CaO:ZrO_2-based MIM structures were measured. Thirty tested devices for each composition of CaO:ZrO_2 film were measured to obtain the average values of conductivity. Agilent 4155C semiconductor parameter analyzer was used to measure the current–voltage (I–V) curves. Agilent 81110A was employed to generate voltage pulses to change the memory states of the device, followed by Agilent 4155C verification.

III. Results and Discussion

The cross-sectional transmission electron microscopy (TEM) image in the inset of Fig. 1(a) shows that an approximately 5-nm-thick 2-mol% CaO:ZrO_2 buffer layer replaces the original ZrO_y layer. Fig. 1(a) reveals the typical RS behavior in the Ti/2-mol% CaO:ZrO_2/ZrO_2/Pt device, where a -8-V forming voltage with 5-mA current compliance is required before performing any RS (not shown here). After the forming process, the voltage is swept to -1.3 V without any current compliance, and the current abruptly drops. This means that the device is switched from ON state to OFF state. An abrupt current increase occurs when the voltage is swept to -3 V with 5-mA current compliance, and OFF state is switched back to ON state. The inset in Fig. 1(a) indicates the result of tracing continuous RS cycles over 400 times, where both ON and OFF states are stable without any RS operation failure. Fig. 1(b) shows a statistical chart of the endurance cycles for the Ti/CaO:ZrO_2/ZrO_2/Pt devices with 0- to 2.8-mol% CaO dopants. Increasing the CaO concentration up to 2 mol% increases the endurance cycle but decreases when the CaO concentration is 2.8 mol% ($\sim 5 \times 10^{19}/\mathrm{cm}^3$).

Taking the site, mass, and charge balances into account, the possible defect equation is expressed as follows [10]:

$$\mathrm{CaO} \xrightarrow{\mathrm{ZrO2}} Ca_{\mathrm{Zr}}^{''} + V_O^{\bullet\bullet} + O_O^{\times} \quad (1)$$

where $\xrightarrow{\mathrm{ZrO2}}$ stands for CaO dopants within ZrO_2; $Ca_{\mathrm{Zr}}^{''}$ denotes calcium ion with doubly negative charge at Zr site; $V_O^{\bullet\bullet}$ indicates oxygen vacancy with doubly positive charge; and $O_O^{\times}$ represents oxygen ion on its own lattice site, which is neutral. Therefore, 1 mol of CaO dopant creates 1 mol of oxygen vacancy within ZrO_2. Fig. 1(c) shows the electrical conductivity of the CaO:ZrO_2 buffer layer at room temperature (RT), and there is maximum conductivity occurred at 2-mol% CaO concentration. The 2.8-mol% CaO:ZrO_2 layer has a lower conductivity value than the 2-mol% CaO:ZrO_2 layer. This phenomenon might be attributed to the formation of defect associations due to the higher concentration of $Ca_{\mathrm{Zr}}^{''}$ and $V_O^{\bullet\bullet}$ in the 2.8-mol% layer [10]. The conduction mechanism also consists with Poole–Frenkel emission at temperatures ranging from 298 K to 373 K (not shown here).

During the RS process, a large amount of current induces Joule heating, producing a high temperature ($>$ 700 K) to increase the reduction/reoxidation rate in certain regions of the conducting filament [11]. Consequently, in such a high-temperature condition, the CaO:ZrO_2 buffer layer is believed to have higher oxygen ion conductivity. Oxygen ion conductivity σ_i ($\sigma_i = q_i \mu_i c_i$, where q_i is the charge, μ_i is the oxygen ion mobility, and c_i is the charge carrier density) can be expressed as [10]

$$\sigma_i = 2\mu_o c_i T^{-1} \exp\left[-\frac{E_\mu}{kT}\right] \quad (2)$$

where $\mu_o (= qi^2 Do/2k)$ is constant, D_o is a diffusion coefficient related to material property, T is temperature, E_μ is the activation energy of the oxygen vacancy diffusion, and k is Boltzmann's constant. The higher CaO doping concentration creates more oxygen vacancies [see (1)], leading to higher c_i and smaller E_μ (resultantly higher σ_i). Moreover, the CaO doping concentration affects σ_i of CaO:ZrO_2 bulk ceramics by two to three orders of magnitude [12]. Compared with the native ZrO_y layer, σ_i of the 2-mol% CaO:ZrO_2 buffer layer is assumed to be raised more than two orders of magnitude. Under the same operation duration, more than 100 times, the oxygen ions move from the TiO_z layer laterally and vertically across the 2-mol% CaO:ZrO_2 buffer layer to the interface between the CaO:ZrO_2 and ZrO_2 layers, where the formation and rupture of the conducting filament occur. More oxygen ions can effectively form and rupture the conducting filament. Therefore, the Ti/2-mol% CaO:ZrO_2/ZrO_2/Pt device exhibits more endurance cycles.

Figs. 2(a) and (b) show the dynamic pulse operations of the Ti/ZrO_2/Pt (with 0-mol% CaO concentration) and the Ti/2-mol% CaO:ZrO_2/ZrO_2/Pt devices, respectively. The dynamic pulse operation is described as follows. By applying a -4-V 50-ns voltage pulse on the Ti top electrode of the device, the memory state is switched from ON state to OFF state. Then, it is switched back to ON state by applying a -6-V 50-ns voltage pulse. The ON-state and OFF-state current is measured at -0.3 V. The Ti/ZrO_2/Pt device exhibits some soft errors during the dynamic pulse operation. However, the Ti/2-mol% CaO:ZrO_2/ZrO_2/Pt device shows no soft errors. Therefore, by introducing the 2-mol% CaO:ZrO_2 buffer layer, more oxygen

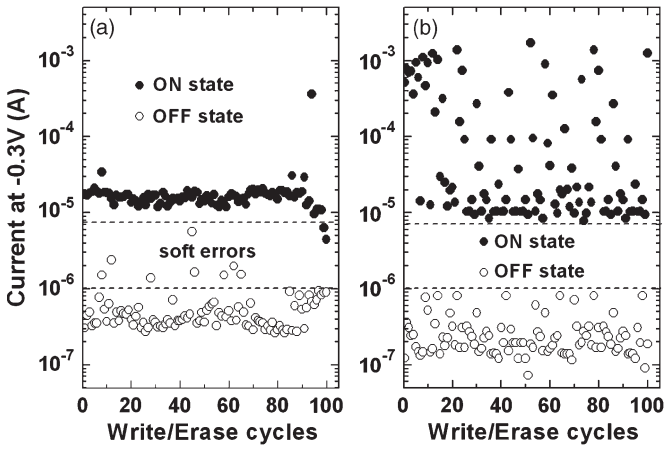

Fig. 2. RS cycles of (a) the Ti/ZrO_2/Pt and (b) the Ti/2-mol% CaO:ZrO_2/ZrO_2/Pt devices by applying dynamic pulses. Applying a −6-V 50-ns pulse to switch the memory state to ON state and applying a −4-V 50-ns pulse to switch back to OFF state.

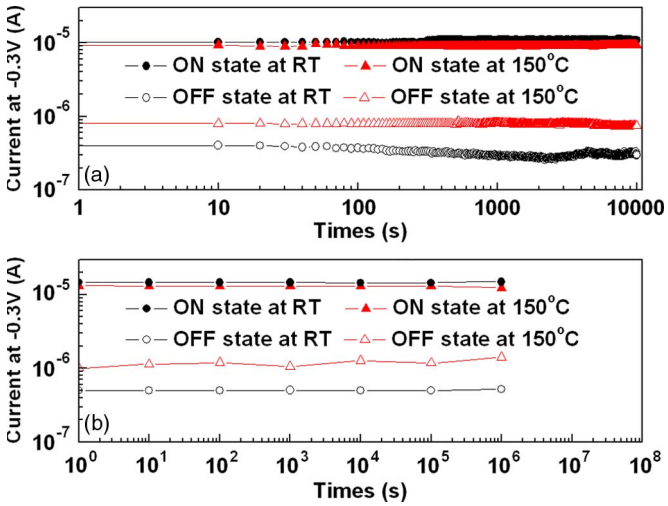

Fig. 3. (a) Nondestructive readout properties and (b) retention characteristics of the Ti/CaO:ZrO_2/ZrO_2/Pt device at RT and 150 °C.

ions are available from the TiO_z layer laterally and vertically to form and rupture the conducting filament. Figs. 3(a) and (b) respectively demonstrate the nondestructive readout properties and retention characteristics of the device to further evaluate its memory performance. Results show that both ON and OFF states are stable at RT and 150 °C, respectively. Further research is necessary to investigate the scalability of the device (including film thickness and cell size) and the 1T1R architecture to understand whether the Ti/2-mol% CaO:ZrO_2/ZrO_2/Pt device is a reliable memory device for next-generation nonvolatile memory applications.

IV. Conclusion

Replacing the native ZrO_y layer of a ZrO_2-based memory device with an artificial CaO:ZrO_2 oxygen ion conductor buffer layer improves its RS properties. The 2-mol% CaO doping concentration creates more oxygen vacancies within the CaO:ZrO_2 buffer layer, thus enhancing its oxygen ion conductivity. Under the same operation duration, more oxygen ions migrate from the TiO_z layer laterally and vertically across the 2-mol% CaO:ZrO_2 buffer layer to form and rupture the conducting filament. The Ti/2-mol% CaO:ZrO_2/ZrO_2/Pt device exhibits more endurance cycles and no soft errors. For nondestructive readout and retention, both ON and OFF states remain stable at both RT and 150 °C. This letter has shown that the oxygen ion conductivity of the interface layer between the top electrode and the RS film significantly improves the unipolar RS properties of ZrO_2-based memory devices.

References

[1] C. Y. Lin, C. Y. Wu, C. Y. Wu, T. C. Lee, F. L. Yang, C. Hu, and T. Y. Tseng, "Effect of top electrode material on resistive switching properties of ZrO_2 film memory devices," *IEEE Electron Device Lett.*, vol. 28, no. 5, pp. 366–368, May 2007.

[2] D. C. Kim, M. J. Lee, S. E. Ahn, S. Eso, J. C. Park, I. K. Yoo, I. G. Baek, H. J. Kim, E. K. Yim, J. E. Lee, S. O. Park, H. S. Kim, U. I. Chung, J. T. Moon, and B. I. Ryu, "Improvement memory switching in NiO using IrO_2," *Appl. Phys. Lett.*, vol. 88, no. 23, pp. 232106-1–232106-3, Jun. 2006.

[3] H. Y. Lee, P. S. Chen, T. Y. Wu, Y. S. Chen, C. C. Wang, P. J. Tzeng, C. H. Lin, F. Chen, C. H. Lien, and M. J. Tsai, "Low power and high speed bipolar switching with a thin reactive Ti buffer layer in robust HfO_2 based RRAM," in *IEDM Tech. Dig.*, 2008, pp. 297–300.

[4] S. Y. Wang and T. Y. Tseng, "Interface engineering in resistive switching memories," *J. Adv. Dielectr.*, vol. 1, no. 2, pp. 141–162, Apr. 2011.

[5] K. M. Kim, B. J. Choi, and C. S. Hwang, "Localized switching mechanism in resistive switching of atomic-layer-deposited TiO_2 thin films," *Appl. Phys. Lett.*, vol. 90, no. 24, pp. 242906-1–242906-3, Jun. 2007.

[6] D. Y. Lee, S. Y. Wang, and T. Y. Tseng, "Ti-induced recovery phenomenon of resistive switching in ZrO_2 thin films," *J. Electrochem. Soc.*, vol. 157, no. 7, pp. G166–G169, May 2010.

[7] S. Y. Wang, D. Y. Lee, T. Y. Tseng, and C. Y. Lin, "Effects of Ti top electrode thickness on the resistive switching behaviors of rf-sputtered ZrO_2 memory films," *Appl. Phys. Lett.*, vol. 95, no. 11, pp. 112904-1–112904-3, Sep. 2009.

[8] C. Y. Lin, C. Y. Wu, C. Y. Wu, C. Hu, and T. Y. Tseng, "Modified resistive switching behavior of ZrO_2 memory films based on the interface layer formed by using Ti top electrode," *J. Appl. Phys.*, vol. 102, no. 9, pp. 094101-1–094101-5, Nov. 2007.

[9] G. H. Kim, J. H. Lee, J. Y. Seok, S. J. Song, J. H. Yoon, K. J. Yoon, M. H. Lee, K. M. Kim, H. D. Lee, S. W. Ryu, T. J. Park, and C. S. Hwang, "Improved endurance of resistive switching TiO_2 thin film by hour-glass shaped Magnéli filaments," *Appl. Phys. Lett.*, vol. 98, no. 26, pp. 262901-1–262901-3, Jun. 2011.

[10] Y. M. Chiang, D. B. III, and W. D. Kingery, *Physical Ceramic: Principles for Ceramic Science and Engineering*. New York: Wiley, 1997.

[11] Y. Sato, K. Kinoshita, M. Aoki, and Y. Sugiyama, "Consideration of switching mechanism of binary metal oxide resistive junctions using a thermal reaction model," *Appl. Phys. Lett.*, vol. 90, no. 3, pp. 033503-1–033503-3, Jan. 2007.

[12] T. Y. Tien, "Electrical conductivity in the system ZrO_2-$CaZrO_3$," *J. Amer. Ceram. Soc.*, vol. 47, no. 9, pp. 430–433, Sep. 1964.